min), a ~100 nM solution of biotinylated red nanocrystals (30 min), again streptavidin (30 min), then once more with the red biotinylated nanocrystals (30 min). At least three PBS or Superblock-PBS (Pierce) rinse steps (5 min each) were performed between each incubation. Samples were mounted on microscope slides in PBS.

28. We would like to thank X. Peng, J. Gray, C. Bertozzi, and P. Schultz for many helpful discussions. The photoluminescence spectra of InAs nanocrystals, InP nanocrystals, and CdSe nanocrystals in Fig. 2 were provided by J. Wickham, U. Banin, and X. Peng. Supported by the Director, Office of Energy Research, Office of Basic Energy Sciences, Division of Materials Sciences, of the U.S. Department of Energy under contract number DE-AC03-76SF00098. M.B. acknowledges support from a NSF graduate research fellowship.

27 May 1998; accepted 20 August 1998

# Quantum Dot Bioconjugates for Ultrasensitive Nonisotopic Detection

**Warren C. W. Chan and Shuming Nie***

**Highly luminescent semiconductor quantum dots (zinc sulfide–capped cadmium selenide) have been covalently coupled to biomolecules for use in ultrasensitive biological detection. In comparison with organic dyes such as rhodamine, this class of luminescent labels is 20 times as bright, 100 times as stable against photobleaching, and one-third as wide in spectral linewidth. These nanometer-sized conjugates are water-soluble and biocompatible. Quantum dots that were labeled with the protein transferrin underwent receptor-mediated endocytosis in cultured HeLa cells, and those dots that were labeled with immunomolecules recognized specific antibodies or antigens.**

The development of sensitive nonisotopic detection systems has substantially impacted many research areas, such as DNA sequencing, clinical diagnostics, and fundamental molecular biology (*1*). These systems aim to solve the problems of radioactive detection (for example, health hazards and short lifetimes) and open new possibilities in ultrasensitive and automated biological assays. Current nonisotopic detection methods are mainly based on organic reporter molecules that undergo enzyme-linked color changes or that are fluorescent, luminescent, or electroactive (*1*). We have developed a class of nonisotopic detection labels by coupling luminescent semiconductor quantum dots (QDs) to biological molecules. In this design, nanometer-sized QDs are detected through photoluminescence, and the attached biomolecules recognize specific analytes, such as proteins, DNA, or viruses. These nanoconjugates are biocompatible and are suitable for use in cell biology and immunoassay. At the present level of development, however, the QDs are not sufficiently monodisperse, and intermittent photon emission could cause statistical problems at the single-dot level.

Molecular conjugates of luminescent QDs are expected to offer substantial advantages over organic dyes. The properties of QDs result from quantum-size confinement, which occurs when metal and semiconductor particles are smaller than their exciton Bohr radii (about 1 to 5 nm) (*2–4*). Recent advances have resulted in the large-scale preparation of relatively monodisperse QDs (*5–7*), the characterization of their lattice structures (*4*), and the fabrication of QD arrays (*8–12*) and light-emitting diodes (*13*, *14*). For example, CdSe QDs passivated with a ZnS layer are strongly luminescent (35 to 50% quantum yield) at room temperature, and their emission wavelength can be tuned from the blue to the red wavelengths by changing the particle size (*7*, *15*). However, these luminescent QDs are prepared in organic solvents and are not suitable for biological application. Additionally, it is unclear how to attach biomolecules to a QD and still maintain their activity.

We have solved these problems by using mercaptoacetic acid for solubilization and covalent protein attachment. When reacted with ZnS-capped CdSe QDs in chloroform, the mercaptoacetic acid, was extracted. Excess mercaptoacetic acid was removed by four or more rounds of centrifugation. The purified QDs were conjugated to transferrin and IgG with the cross-linking reagent ethyl-3-(dimethylaminopropyl)carbodiimide. Standard protocols were followed (*16*), except the excess proteins were removed by repeated centrifugation. The purified conjugates were stored in PBS at room temperature.

Department of Chemistry, Indiana University, Bloomington, IN 47405, USA.

*To whom correspondence should be addressed. E-mail: nie@indiana.edu

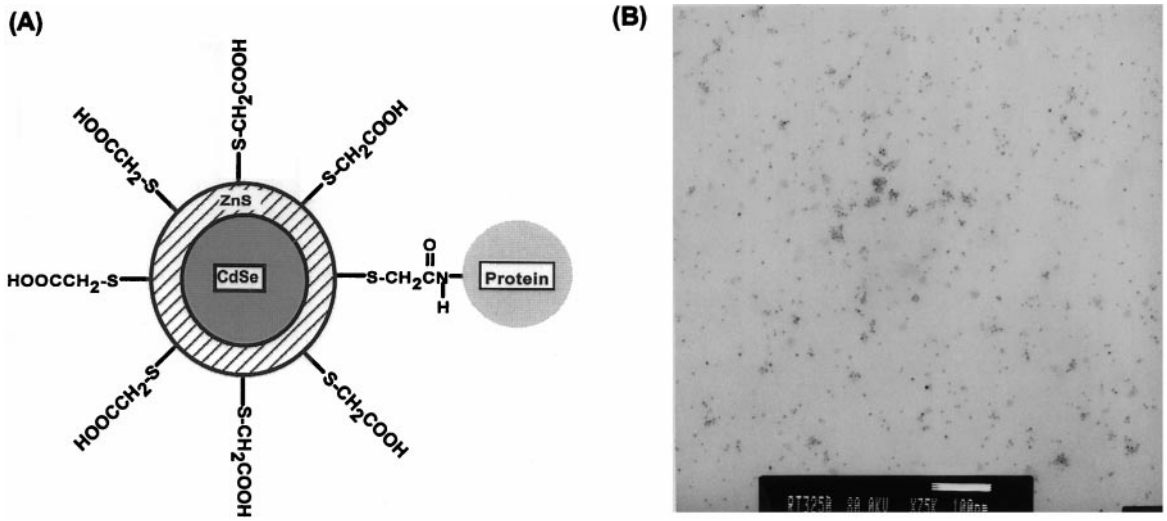


**Fig. 1.** (**A**) Schematic of a ZnS-capped CdSe QD that is covalently coupled to a protein by mercaptoacetic acid. (**B**) TEM of QD-transferrin (an iron-transport protein) conjugates. Scale bar, 100 nm. Clusters of closely spaced particles were mainly formed by sample spreading and drying on the carbon grid and not by chemical cross-linking. ZnS-capped QDs with a CdSe core size of 4.2 nm were prepared according to the procedure developed by Hines and Guyot-Sionnest (*7*). The colloidal QDs were dissolved in chloroform and were reacted with glacial mercaptoacetic acid (~1.0 M) for 2 hours. An aqueous phosphate-buffered saline (PBS) solution (pH 7.4) was added to this reaction mixture at a 1:1 volume ratio. After vigorous shaking and mixing, the chloroform and water layers separated spontaneously. The aqueous layer, which contained mercapto-coated

capto group binds to a Zn atom, and the polar carboxylic acid group renders the QDs water-soluble (Fig. 1A). The free carboxyl group is also available for covalent coupling to various biomolecules (such as proteins, peptides, and nucleic acids) by cross-linking to reactive amine groups (*16*). In addition, this mercaptoacetic acid layer is expected to reduce passive protein adsorption on QDs. Transmission electron microscopy (TEM) (Fig. 1B) showed that the solubilization and cross-linking steps did not result in aggregation and that the QD bioconjugates were primarily single particles. This finding was also supported by ultrasensitive optical measurements at the single-dot level. A comparison of color luminescence images that were obtained from the original QDs, the water-soluble QDs, and the protein-conjugated QDs (Fig. 2) indicated that the optical properties of QDs remain unchanged after solubilization and conjugation. Bulk optical measurements (*17*) also showed that the emission spectra and efficiencies were similar for the original sample (in chloroform) and the water-soluble QDs. The numbers of mercaptoacetic acid and protein molecules per QD have not been determined experimentally. For steric reasons, perhaps only two to five molecules of a 100-kD protein can be attached to a 5-nm QD, which is similar to the number of protein molecules that can be attached to a 5-nm colloidal gold particle (*16*).

Several lines of evidence suggest that the observed luminescence signals resulted from spatially isolated single QDs. First, the measured particle density was consistent with the value that was calculated from the sample volume and concentration. Second, the colloidal QDs were not homogeneous in size (~5% variation), and the bulk sample showed a single broad emission peak (*7*, *15*). However, when individual QDs were examined, discrete luminescence peaks were observed [as seen in a rainbow of luminescence colors (Fig. 2)]. Third, the discrete luminescence signals showed an intermittent on and off behavior, which was similar to the behavior reported for single fluorescent molecules (*16*, *18*–*20*) and single CdSe QDs (*21*, *22*). This "blinking" behavior may seem fascinating from a fundamental point of view but can cause signal intensity fluctuations in ultrasensitive detection. This problem could be overcome by coating QDs with a thicker ZnS layer and by reducing the excitation light intensity (*21*).

We further compared the photophysical properties of the QD conjugates with those of common organic dyes. Wavelength-resolved spectra and time-resolved photobleaching data, which were obtained from single QDs as well as bulk materials, are shown in Fig. 3. The intrinsic QD spectral width [full width at half maximum (FWHM) is 12 nm] is about one-third as wide as that of a fluorescent sphere (FWHM is 35 nm). Furthermore, the QD emission (time constant $t_{1/2}$ = 960 s) is nearly 100 times as stable as rhodamine 6G (R6G) ($t_{1/2}$ = 10 s) against photobleaching. In this approximate comparison of photobleaching rates, the differences between QD and R6G fluorescence quantum yields were not taken into account. Using wavelength-matched fluorescent latex spheres as a standard, we estimated that the fluorescence intensity of a single CdSe QD is equivalent to that of ~20 rhodamine molecules (*23*). This result compares well with that for the fluorescent protein phycoerythrin, which has a fluorescence intensity equivalent to that of 25 R6G molecules but is unstable photochemically (*24*). However, for the QD bioconjugates to be broadly useful in ultrasensitive analysis, the attached biomolecules must be active and must be able to recognize specific analytes in a complex mixture.

With covalently attached proteins, we demonstrated that the QDs were biocompatible in vitro and with living cells. Fluorescence images obtained from cultured HeLa cells that had been incubated with mercapto-QDs (control) and with transferrin-QD bioconjugates are

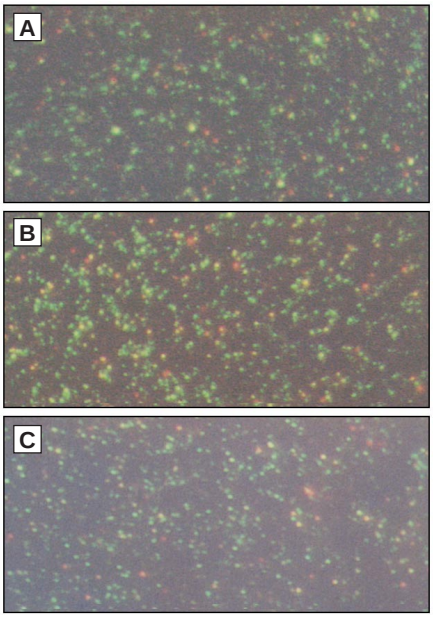


**Fig. 2.** Color luminescence images obtained from (**A**) original QDs, (**B**) mercapto-solubilized QDs, and (**C**) QD-IgG conjugates. The images were directly recorded on color photographic film (ASA-1600) with a 15-s exposure by a 35-mm camera that was attached to a Nikon inverted optical microscope. Samples of dilute QDs were deposited and spread on polylysine-coated glass coverslips, resulting in spatially isolated single QDs on the surface. Continuous-wave excitation at 514.5 nm was provided by an Ar ion laser (Lexel Laser, Fremont, California). A longpass dielectric filter (Chroma Tech, Brattleboro, Vermont) was used to reject the scattered laser light and to pass the Stokes-shifted luminescent photons. A high-numerical-aperture (NA) (1.3), oil-immersion objective was used, and the total laser power at the sample was 50 mW. There are emission color differences among single QDs.

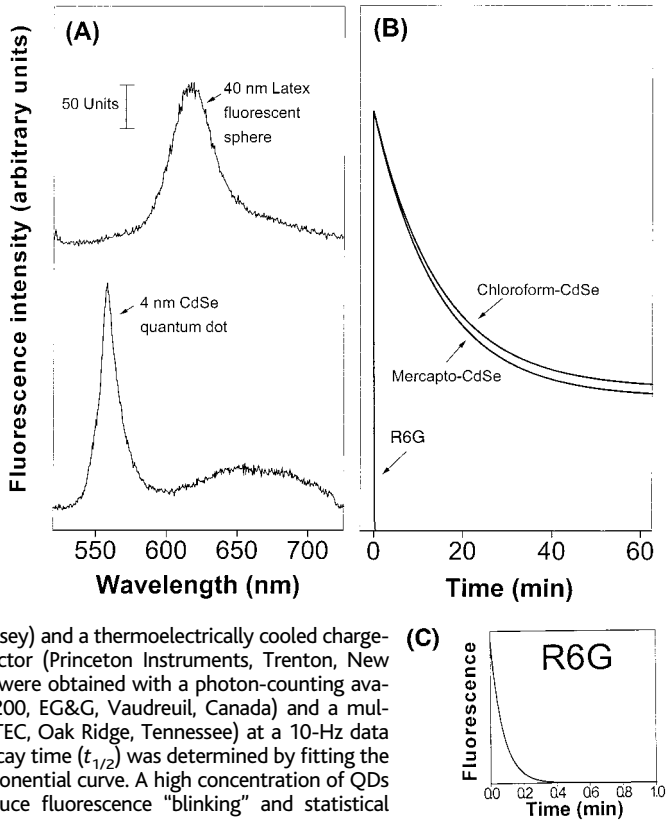


**Fig. 3.** Comparison of the photophysical properties of luminescent QDs and organic dyes. (**A**) Wavelength-resolved spectra obtained from a single 40-nm fluorescent latex sphere and a single mercapto-QD. The broad emission peak at ~660 nm is believed to result from surface defects on the QD. (**B**) Time-resolved photobleaching curves for the original QDs, the solubilized QDs, and the dye R6G. (**C**) The time-resolved photobleaching curve for R6G is shown in detail. Single-particle spectroscopy was performed with a confocal fluorescence microscope that was attached to a single-stage spectrograph (Model 270M, Spex, Edison, New Jersey) and a thermoelectrically cooled charge-coupled device (CCD) detector (Princeton Instruments, Trenton, New Jersey). Time-resolved data were obtained with a photon-counting avalanche photodiode (SPCM-200, EG&G, Vaudreuil, Canada) and a multichannel scalar (EG&G ORTEC, Oak Ridge, Tennessee) at a 10-Hz data acquisition rate. The half-decay time ($t_{1/2}$) was determined by fitting the experimental data to an exponential curve. A high concentration of QDs and R6G was used to reduce fluorescence "blinking" and statistical fluctuation.

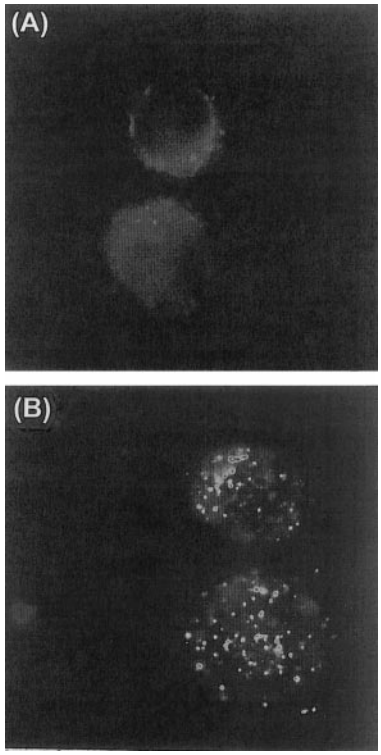


**Fig. 4.** Luminescence images of cultured HeLa cells that were incubated with (**A**) mercapto-QDs and (**B**) QD-transferrin conjugates. The QD bioconjugates were transported into the cell by receptor-mediated endocytosis and were detected as clusters or aggregates. Luminescence "blinking" was not observed for these clusters because of statistical averaging. The images were obtained with an epifluorescence microscope that was equipped with a high-resolution CCD camera (1.4 million pixels) (Photometrix, Tucson, Arizona) and a 100-W Hg excitation lamp. HeLa cells were grown in a minimum essential medium containing 10% fetal calf serum, 1% antibiotics (penicillin and streptomycin), and fungizone. The cultured cells were incubated overnight with either control QDs or the transferrin conjugates at 37°C. After repeated washings to eliminate excess QDs, the cells were removed from the petri dish and placed on a glass cover slip for imaging. The trypsin-treated cells had a spherical shape on the cover slip. Cell diameter, ~10 μm.

shown in Fig. 4. In the absence of transferrin, no QDs were observed inside the cell, and the image resulted from weak cellular autofluorescence. When transferrin was present, receptor-mediated endocytosis occurred, and the luminescent QDs were transported into the cell (*25*). Clearly, the attached transferrin molecules were still active and were recognized by the receptors on the cell surface. As with nanometer-sized colloidal gold, the QD labels did not substantially interfere with ligand-receptor binding or endocytosis.

We also investigated the suitability of QD labels for sensitive immunoassay. The fluorescence images of QD–immunoglobulin G (IgG) conjugates that were incubated with

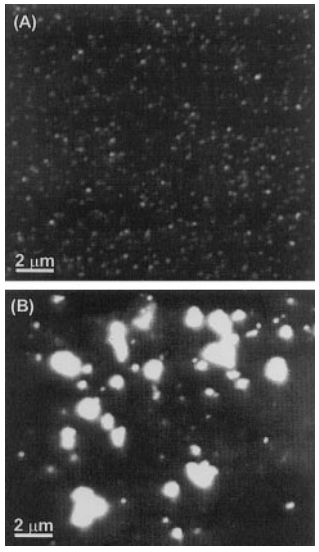


**Fig. 5.** Antibody-induced agglutination of QDs that were labeled with human IgG. (**A**) Luminescence image of QD conjugates in the presence of BSA (0.5 mg/ml). (**B**) Luminescence image of aggregated QDs induced by a specific polyclonal antibody (0.5 μg/ml).

bovine serum albumin (BSA) (0.5 mg/ml) and with a specific polyclonal antibody (0.5 μg/ml) are shown in Fig. 5. The polyclonal antibody recognized the Fab fragments of the immunoglobulin and led to extensive aggregation of the QDs. In contrast, well-dispersed and primarily single QDs were detected in the presence of BSA (*26*). This simple experiment showed that the attached immunomolecules can recognize specific antibodies or antigens. The observed aggregation of QDs was similar to latex immunoagglutination, which is a technique that is widely used in clinical diagnostics (*27*).

In conclusion, semiconductor QDs have been covalently attached to biomolecules for ultrasensitive detection at the single-dot level. We envision that the improved photostability could allow real-time observations of ligand-receptor interaction and of molecular trafficking in living cells. Also, current combinatorial labeling with traditional organic dyes allows only 25 DNA sequences to be detected simultaneously (*28*). Further synthetic efforts may produce sufficiently monodispersed QDs (*29*), which should be important toward developing multiplexed detection schemes. When combined with sandwich immunoassay or nucleic acid hybridization, the use of QD probes should open new possibilities in detecting single native biomolecules, such as cytokines and viral RNA.

### References and Notes

1. For recent books, see L. J. Kricka, Ed., *Nonisotopic Probing, Blotting, and Sequencing* (Academic Press, New York, 1995); P. G. Issac, Ed., *Protocols for Nucleic Acid Analysis by Nonradioactive Probes* (Humana, Totowa, NJ, 1994); E. P. Diamandis and T. K. Christopoulos, Eds., *Immunoassay* (Academic Press, New York, 1996).
2. A. P. Alivisatos, *Science* **271**, 933 (1996); *J. Phys. Chem.* **100**, 13226 (1996).
3. L. E. Brus, *Appl. Phys. A* **53**, 465 (1991); W. L. Wilson, P. F. Szajowski, L. E. Brus, *Science* **262**, 1242 (1993).
4. A. Henglein, *Chem. Rev.* **89**, 1861 (1989); H. Weller, *Angew. Chem. Int. Ed. Engl.* **32**, 41 (1993).
5. C. B. Murray, D. J. Norris, M. G. Bawendi, *J. Am. Chem. Soc.* **115**, 8706 (1993).
6. J. E. Bowen Katari, V. L. Colvin, A. P. Alivisatos, *J. Phys. Chem.* **98**, 4109 (1994).
7. M. A. Hines and P. Guyot-Sionnest, *ibid.* **100**, 468 (1996).
8. C. B. Murray, C. R. Kagan, M. G. Bawendi, *Science* **270**, 1335 (1995).
9. R. P. Andres *et al.*, *ibid.* **273**, 1690 (1996).
10. J. R. Heath *et al.*, *J. Phys. Chem.* **100**, 3144 (1996); C. P. Collier, R. J. Saykally, J. J. Shiang, S. E. Henrichs, J. R. Heath, *Science* **277**, 1978 (1997).
11. C. A. Mirkin, R. L. Letsinger, R. C. Mucic, J. J. Storhoff, *Nature* **382**, 607 (1996).
12. A. P. Alivisatos *et al.*, *ibid.*, p. 609.
13. V. L. Colvin, M. C. Schlamp, A. P. Alivisatos, *ibid.* **370**, 354 (1994).
14. B. O. Dabbousi, M. G. Bawendi, O. Onotsuka, M. F. Rubner, *Appl. Phys. Lett.* **66**, 1316 (1995).
15. B. O. Dabbousi *et al.*, *J. Phys. Chem. B* **101**, 9463 (1997).
16. G. T. Hermanson, *Bioconjugate Techniques* (Academic Press, New York, 1996).
17. W. C. W. Chan and S. Nie, unpublished data.
18. R. M. Dickson, A. B. Cubitt, R. Y. Tsien, W. E. Moerner, *Nature* **388**, 355 (1997).
19. H. P. Lu and X. X. Xie, *ibid.* **385**, 143 (1997).
20. D. A. Vanden *et al.*, *Science* **277**, 1074 (1997).
21. M. Nirmal *et al.*, *Nature* **383**, 802 (1996); S. A. Empedocles, D. J. Norris, M. G. Bawendi, *Phys. Rev. Lett.* **77**, 3873 (1996).
22. S. A. Blanton, M. A. Hines, P. Guyot-Sionnest, *Appl. Phys. Lett.* **69**, 3905 (1996).
23. The 40-nm fluorescent latex spheres ($\lambda_{ex}$ = 530 nm; $\lambda_{em}$ = 560 nm) ($\lambda_{ex}$, excitation wavelength maximum; $\lambda_{em}$, emission wavelength maximum) were purchased from Molecular Probes (Eugene, OR). Each sphere is equivalent in intensity to ~350 dye molecules [R. P. Haugland, *Handbook of Fluorescent Probes and Research Chemicals* (Molecular Probes, Eugene, OR, ed. 6, 1995)]. The integrated emission intensities for single QDs and single latex spheres were measured and compared under identical experimental conditions. The single-dot photoluminescence was about one-seventeenth that of a single latex sphere and thus was estimated to be equal to the total emission intensity of 20 R6G molecules.
24. K. Peck, L. Stryer, A. N. Glazer, R. A. Mathies, *Proc. Natl. Acad. Sci. U.S.A.* **86**, 4087 (1989).
25. D. A. Edwards, K. J. Gooch, I. Zhang, G. H. McKinley, R. Langer, *ibid.* **93**, 1786 (1996); E. Smythe and G. Warren, *Eur. J. Biochem.* **202**, 689 (1991).
26. Quantitative measurements showed that the intensity variations among the discrete luminescent signals were within a factor of 3. Thus, the observed signals arose primarily from single QDs and, perhaps, a small population of double- and triple-dot aggregates. Protein BSA should adsorb nonspecifically on the QDs, but it did not cause particle aggregation.
27. L. B. Bangs, *Pure Appl. Chem.* **68**, 1873 (1996).
28. M. R. Speicher, S. G. Ballard, D. C. Ward, *Nature Genet.* **12**, 368 (1996).
29. X. Peng, J. Wickman, A. P. Alivisatos, *J. Am. Chem. Soc.* **120**, 5343 (1998).
30. We are grateful to M. A. Hines and P. Guyot-Sionnest for their help in QD synthesis and for providing the original ZnS-capped CdSe sample. We also thank A. K. Reuter for bulk optical measurement, R. Turner for TEM, and S. R. Emory for valuable discussions. This work was supported in part by NSF grant CHE-9610254 and by the Petroleum Research Fund grant 32231-AC5. S.N. acknowledges the Whitaker Foundation for a Biomedical Engineering Award and the Beckman Foundation for a Beckman Young Investigator Award.

17 June 1998; accepted 27 August 1998

# Quantum Dot Bioconjugates for Ultrasensitive Nonisotopic Detection

Warren C. W. Chan and Shuming Nie

*Science* **281** (5385), 2016-2018.
DOI: 10.1126/science.281.5385.2016